Generalized Core and Winding Area Ratio - Trends for Inductors and Transformers in Power Electronics with High Switching Frequencies

Siqi Lin[1], Leon Fauth[1], Wilmar Martnez[2], and Jens Friebe[1]
[1]Leibniz Universitat Hannover
[2]KU Leuven - Energyville
[1]Welfengarten - Hannover, Germany
[2]Diepenbeek - Genk, Belgium
Phone: +49 (0) 511 762 19477
Email: siqi.lin@ial.uni-hannover.de
URL: http://www.ial.uni-hannover.de

Keywords

≪Power Electronics≫, ≪Core area≫, ≪Winding area≫, ≪Inductors≫, ≪Transformers≫ .

Abstract

The paper describes the general trend for the design of core shapes for inductors and transformers in power electronic applications under the influence of increasing switching frequencies. The focus of the paper is on the ratio of the winding window and the core cross sectional area to identify the current trends and new shapes for magnetic circuits.

Introduction

Design of magnetic core components in power electronics is distinctly unique, which means that the magnetic designers need to design magnetic components specifically for each application. With the increasing use of wide-bandgap-semiconductors the high frequency losses of magnetic components become a major factor that limits the power density as well as the efficiency to be further improved. On the one hand coil losses have to be limited by different high frequency coil forms as well as winding arrangements [1] [2], on the other hand the size of the core should be constrained to avoid eddy current effects and dimensional resonance effects in the core caused by high frequencies and the material properties [3] [4]. This requires the magnetic designer to find a balance between the winding arrangement and the core cross section area. This paper shows the trend of core geometry in the case of high frequency power electronics by examining the ratio of winding window to core cross section, and giving a general approach for selecting or judging core geometry.

The most common method of core geometry selection is the A_p area product method. (1) shows the general A_p method for transformers [5] [6] with output power $P\mathrm{t}$, copper filling factor k_cu and waveform factor k_f etc. It can be seen by (1) that the A_p value is decreasing as the frequency increases, which is in accordance with the law of electromagnetic induction and also roughly demonstrates the ability of the core to handle power at different frequencies.

$$A_\mathrm{p} = A_\mathrm{e} \cdot A_\mathrm{w} = \frac{P\mathrm{t} \cdot 10^4}{k_\mathrm{f} \cdot k_\mathrm{cu} \cdot J \cdot f \cdot B_\mathrm{m}} \tag{1}$$

There might be many cores with similar A_p value, but this information is not enough to help determine the shape of a specific core. The proportion of A_e and A_w occupied in the power transfer during the frequency change still needs to be clarified. According to (1), and using the ferrite material N87 [7] as an

example, the trend of the winding window area A_w over the core cross section A_e can be obtained while the relative core loss is kept at 100 mW/cm³. For the same frequency, the relationship between A_e and A_w can be calculated with constant A_p (Fig. 1). Fig. 1(a) shows that the core demand for the winding window area decreases as the frequency increases, which also means that the ratio of the core cross section area to the winding window area increases as the frequency increases (Fig. 1(b)). It can be inferred from Fig. 1 that as the frequency increases, a larger core cross section area and a smaller winding window area are required. In the next chapter the design of a transformer for a 10 kW series resonant converter will be used as an example to illustrate how the transformer loss varies with the A_e/A_w t different frequencies to determine whether the above inference holds true.

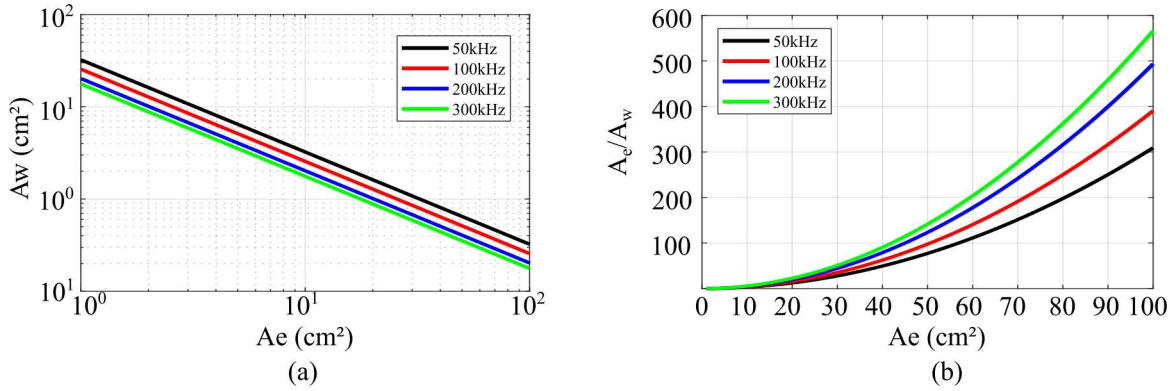

Fig. 1: The trend of core geometry at different frequencies. (a) Trend of variation of window area A_w with core cross-sectional area A_e. (b) Trend of variation of ratio A_e/A_w with core cross section area A_e

.

Analytical calculation

Table I shows the specifications of the design requirements. It is worth noting that it is not intended to design and optimize a transformer here, but only to show the trend of the core geometry change through this example, thus the calculations are simplified accordingly. The core losses are calculated by the steinmetz equation [8] and the coil losses are calculated by the Dowell equation [9].

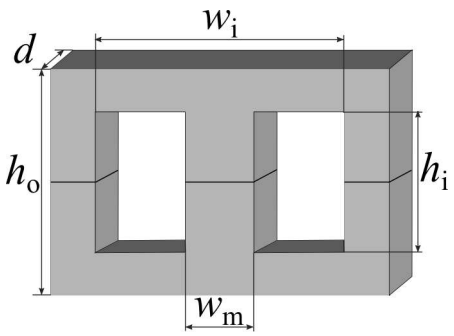

Fig. 2: Core geometry EE core as calculation example. To simplify the calculation, it is assumed that the core geometry satisfies the following relationship: w_i equals three times w_m.

.

$$A_e = d \cdot w_m \tag{2}$$

$$A_w = h_i \cdot w_m \tag{3}$$

(4) shows the actual geometric significance of A_e/A_w for EE-type cores.

$$A_p = A_e \cdot \frac{A_e}{A_w} = \frac{d}{h_i} \tag{4}$$

Table I: DESIGN SPECIFICATIONS FOR TRANSFORMERS

Output Power (W)	Primary Voltage (V)	Secondary Voltage (V)	Duty Cycle	Current Density (A/cm^2)	k_f	k_{cu}
10000	400	400	0.5	420	4	0.4

In Fig. 2, the size parameters of an EE core are shown as example. In the case of the EE type core, the individual side lengths of the core satisfy the following relationship ((2) and (3)) with the winding window area and cross section area.

Fig. 3 shows the commonality of the loss variation at all frequencies. As A_e/A_w increases, the coil loss decreases, but the decrease tends to be flat. The core loss increases as A_e/A_w increases. In order to fairly compare the degree of influence of A_e and A_w on the loss, the specific loss of the core and the type of coil (lize wire) are assumed the same at the same frequency. Since the core geometry is varied in three dimensions, the side length of the center column w_m must also be taken into account although it is known through (4) that w_m does not affect the ratio, but it does affect the coil losses and magnetic losses in different degrees.

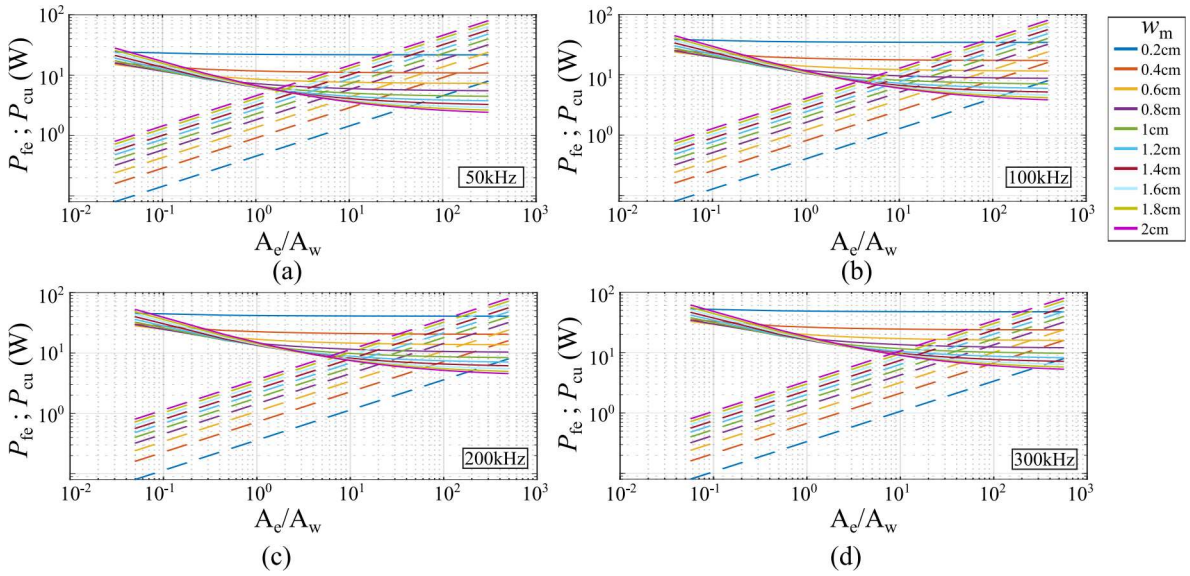

Fig. 3: The trend of core loss and copper loss with ratio A_e/A_w at different frequencies. The solid line is the coil loss and the dashed line is the core loss.

.

Fig. 4 shows the trend of the total transformer losses with frequency, ratio A_e/A_w and side length of the center column w_m. Each frequency corresponds to a case where the total loss is minimized. The ratios A_e/A_w are 0.78, 2, 2.46, and 4.6 for frequencies of 50 kHz, 100 kHz, 200 kHz, and 300 kHz, respectively.

For fixed frequency it is clear that the ratio A_e/A_w is not as large as it should be, the total loss decreases first as the ratio increases and then increases after reaching a minimum value. This is due to the fact that at first the coil loss decreases significantly as the ratio increases, and then tends to smooth out until the decrease in coil loss is compensated by the increase in core loss.

However, as the frequency increases, the trend in loss with ratio shows a tendency to gradually shift to the right side. This means that the core tends to have a larger cross section area and a smaller window area at high frequencies.

Numeric Verification

In order to verify the calculation results of the previous section, 2D finite element simulations have been used. Table II shows the simulation results of core losses. In order to avoid that the errors in the

Table II: 2D FEM TRANSFORMER LOSS SIMULATION RESULTS FOR DIFFERENT FREQUENCIES AND RATIOS.

	50 kHz			100 kHz			200 kHz			300 kHz		
	UO	OP	OO	UO	OP	OO	UO	OP	OO	UO	OP	OO
A_e/A_w	0.28	**0.78**	5.3	0.35	**2**	11.5	0.45	**2.46**	18	0.5	**4.6**	13
P_{total}/W	25	22	25	24.6	21	25.5	34	22	25	50	36	41

calculation and simulation affect the results of the comparison, the tolerance regions of the calculation are defined, as shown in the red areas of Fig. 4, and they represent the minimum regions of the total loss (range of 5% greater than the minimum value). UO, OP, and OO in Table II represent random cases located to the left side, inside, and right side of the loss-minimizing region (red region in Fig. 4), respectively. Meanwhile in Fig. 4 the ratios of PQ40/40 and EILP43 are shown as examples. As shown in the figure, as the frequency increases the distance between PQ40/40 and the loss minimum ratio gets increasingly farther, while the ratio of EILP43 gets closer.

As can be seen in Table II, the trends of 2D FEM simulation results are in agreement with the calculated results. In addition, Fig. 5 visualizes the 3D geometric model of the OP cases at different frequencies. As shown in the Fig. 5, the core decreases significantly in the z-direction and increases in the xy-plane as the frequency increases.

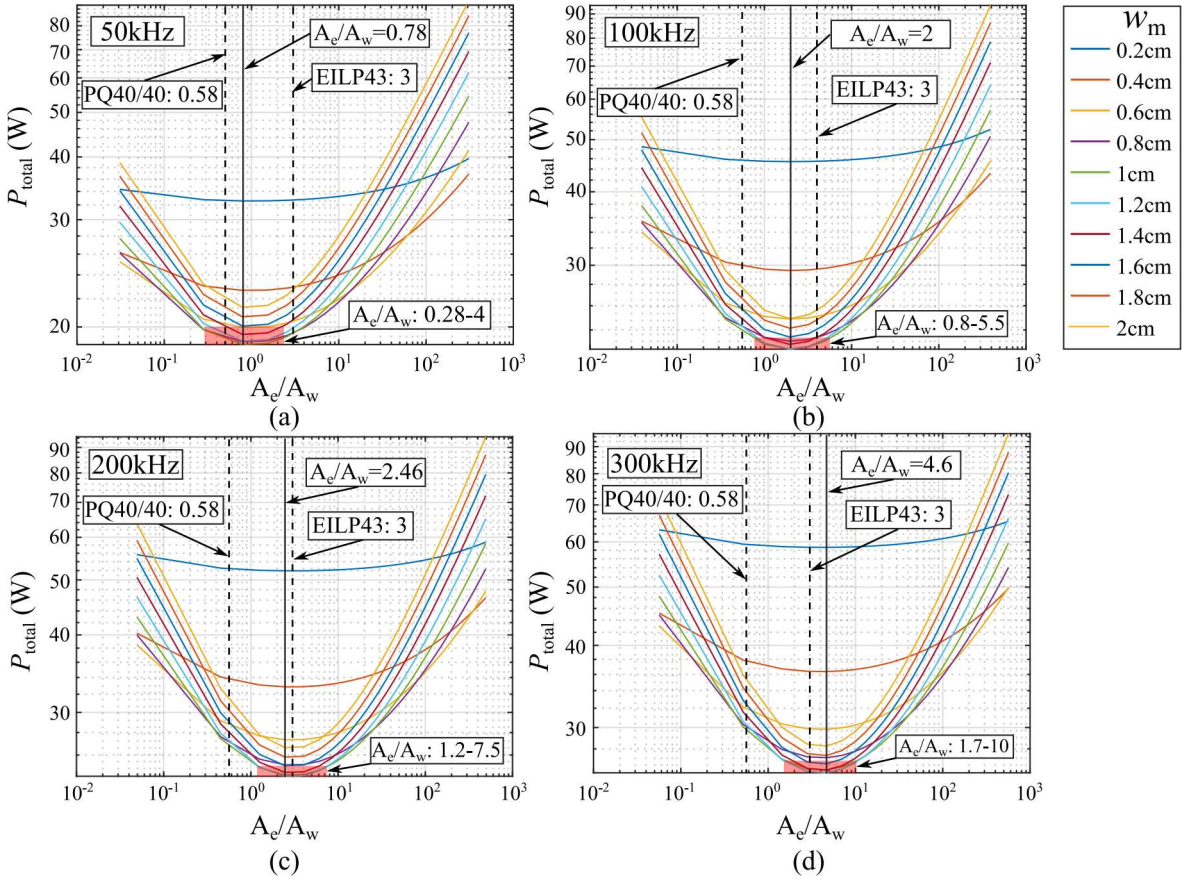

Fig. 4: Trend diagram of transformer losses with ratio A_e/A_w and side length w_m of the center column at different frequencies ((a), (b), (c), and (d) correspond to frequencies 50 kHz, 100 kHz, 200 kHz, and 300 kHz, respectively). The red area shows the range of the ratio A_e/A_w when the total losses are at minimum area (range of 5% greater than the minimum value).

.

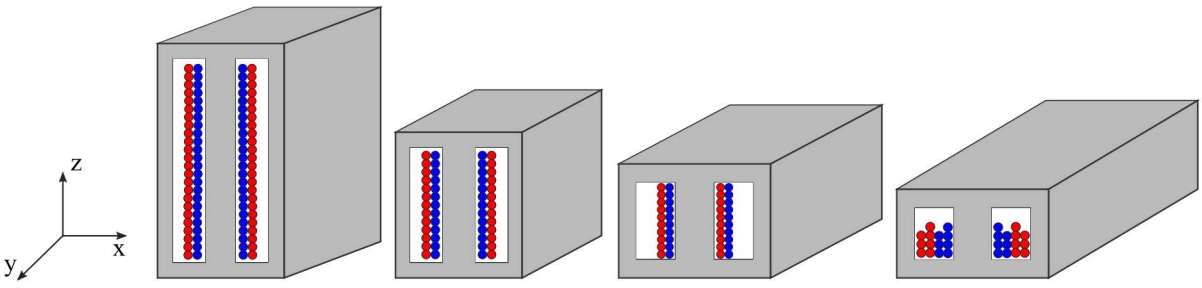

Fig. 5: Comparison of the height of the transformers. a, b, c, and d show the 3D schematic representation models of the variables with the lowest losses at different frequencies (50 kHz, 100 kHz, 200 kHz, and 300 kHz) according to Table I.

.

Measurements

The experimental data were obtained from two 600 W inductors of an ultrasonic converter at 600 kHz, and PQ 40/40 and EILP 43 shapes are used as the cores of the inductor, respectively. Their ratios A_e/A_w are: 0.58 and 3, respectively. The experimental results show that the loss of the inductor using PQ 40/40 is more than 4 W, while using EILP 43 is only about 1 W. In addition, as seen in Fig. 6 a, the new variant (EILP 43) has a significantly lower height and lighter weight. Fig. 6 b shows the inductors being used and the results of the temperature measurements. As shown in the figure, while the maximum temperature of the PQ 40 variant is 83 degrees Celsius, the maximum temperature of the EILP 43 variant is only 52 degrees Celsius. This is because, on the one hand, the EILP 43 variant requires a smaller number of turns due to the increased cross section area of the core, so the coil losses are reduced. On the other hand the flatter surface means better heat dissipation.

Fig. 6: Comparison of inductors for a 600 kHz ultrasonic converter. (a) Prototypes of PQ and EI cores are shown respectively. (b) Temperature measurement results are shown.

.

Conclusion

In this paper, for the first time, the ratio A_e/A_w is used as an indicator to show the trend of the E type core geometry with frequency. As the frequency increases, the larger the ratio, the more advantageous the core is in terms of efficiency, size and heat dissipation. This means that for high frequency magnetic designs, planar cores are preferred. It is because, on the one hand, the exponential growth of coil loss with the increase of frequency, especially for the multi-layer coil arrangement, the coil is severely affected by the proximity effect. Therefore, it is very uneconomical to increase the magnetic parameters by increasing the number of turns. On the other hand, a larger core area provides better heat dissipation. This helps the magnetic designers to determine the specific geometry parameters of the cores and clarify the design direction in the preliminary stage of the design. The research results can also be used as a reference for core manufacturers.

References

[1] A. Stadler and M. Albach, "The influence of the winding layout on the core losses and the leakage inductance in high frequency transformers," in IEEE Transactions on Magnetics, vol. 42, no. 4, pp. 735-738, April 2006, doi: 10.1109/TMAG.2006.871383.

[2] E. L. Barrios, A. Ursúa, L. Marroyo and P. Sanchis, "Analytical Design Methodology for Litz-Wired High-Frequency Power Transformers," in IEEE Transactions on Industrial Electronics, vol. 62, no. 4, pp. 2103-2113, April 2015, doi: 10.1109/TIE.2014.2351786.

[3] E. Cardelli, L. Fiorucci and E. Della Torre, "Estimation of MnZn ferrite core losses in magnetic components at high frequency," in IEEE Transactions on Magnetics, vol. 37, no. 4, pp. 2366-2368, July 2001, doi: 10.1109/20.951174.

[4] G. R. Skutt and F. C. Lee, "Characterization of dimensional effects in ferrite-core magnetic devices," PESC Record. 27th Annual IEEE Power Electronics Specialists Conference, Baveno, Italy, 1996, pp. 1435-1440 vol.2, doi: 10.1109/PESC.1996.548770.

[5] C. W. T. McLyman, Transformer and inductor design handbook. Place of publication not identified: CRC Press, 2017.

[6] C. P. Steinmetz, "The general equations of the electric circuit," in Proceedings of the American Institute of Electrical Engineers, vol. 27, no. 7, pp. 1121-1195, July 1908, doi: 10.1109/PAIEE.1908.6742132.

[7] EPCOS/TDK: Ferrites and accessories material N87, Datasheet, May 2017

[8] P. L. Dowell, "Effects of eddy currents in transformer windings," Proc. Inst. Elect. Eng., vol. 113, no. 8, pp. 1387–1394, Aug. 1966.

[9] R. L. Stoll, The Analysis of Eddy Currents. Oxford, U.K: Clarendon Press, 1974